condensed matter

MDPI

Article

# Structural Evolution of $MoO_3$ Thin Films Deposited on Copper Substrates upon Annealing: An X-ray Absorption Spectroscopy Study

**Salvatore Macis [1,2,*], Javad Rezvani [2], Ivan Davoli [1], Giannantonio Cibin [3], Bruno Spataro [2], Jessica Scifo [2], Luigi Faillace [4] and Augusto Marcelli [2,5]**

1 Department of Physics, Università di Roma Tor Vergata, via della Ricerca Scientifica 1, 00133 Rome, Italy; ivan.davoli@roma2.infn.it
2 Istituto Nazionale Fisica Nucleare, Laboratori Nazionali di Frascati, via Enrico Fermi 40, 00044 Frascati, Italy; Javad.rezvani@lnf.infn.it (J.R.); bruno.spataro@lnf.infn.it (B.S.); jessica.scifo@lnf.infn.it (J.S.); Augusto.Marcelli@lnf.infn.it (A.M.)
3 Diamond Light Source, Harwell Science and Innovation Campus, Didcot OX11 0DE, UK; giannantonio.cibin@diamond.ac.uk
4 Istituto Nazionale Fisica Nucleare, Sezione di Milano, Via Celoria 16, 20133 Milano, Italy; faillax81@gmail.com
5 Rome International Centre for Material Science Superstripes, RICMASS, via dei Sabelli 119A, 00185 Rome, Italy
* Correspondence: salvatore.macis@roma2.infn.it

Received: 14 March 2019; Accepted: 15 April 2019; Published: 18 April 2019


**Abstract:** Structural changes of $MoO_3$ thin films deposited on thick copper substrates upon annealing at different temperatures were investigated via ex situ X-Ray Absorption Spectroscopy (XAS). From the analysis of the X-ray Absorption Near-Edge Structure (XANES) pre-edge and Extended X-ray Absorption Fine Structure (EXAFS), we show the dynamics of the structural order and of the valence state. As-deposited films were mainly disordered, and ordering phenomena did not occur for annealing temperatures up to 300 °C. At ~350 °C, a dominant $\alpha$-$MoO_3$ crystalline phase started to emerge, and XAS spectra ruled out the formation of a molybdenum dioxide phase. A further increase of the annealing temperature to ~500 °C resulted in a complex phase transformation with a concurrent reduction of $Mo^{6+}$ ions to $Mo^{4+}$. These original results suggest the possibility of using $MoO_3$ as a hard, protective, transparent, and conductive material in different technologies, such as accelerating copper-based devices, to reduce damage at high gradients.

**Keywords:** molybdenum; TM oxides; XAFS; thin films

## 1. Introduction

Molybdenum-based oxides are amongst the most adaptable and functional oxides due to their unique characteristics and tunable properties [1–3]. Molybdenum trioxide ($MoO_3$) is one of the thermodynamically stable molybdenum oxides, with the orthorhombic crystal structure $\alpha$-$MoO_3$ [3,4]. The latter phase consists of a set of layers, each one containing distorted $MoO_6$ octahedra, characterized by three different oxygen sites: a single, a double, and a triple shared site. The dipole nature of the $\alpha$-$MoO_3$ layers is at the origin of its relatively high work function (WF) of about 6.5 eV [1,5]. Moreover, despite its insulator nature and high WF, previous studies pointed out that thin $MoO_3$ films may exhibit a conductive behavior in the presence of defects and oxygen vacancies [6–10] or via interaction with a metallic substrate such as copper [7].

$MoO_3$ is used in solar cells, batteries, and organic light-emitting diodes (OLEDs), and it is a promising material for protective coatings of accelerating radiofrequency (RF) cavities [5]. In fact,

due to the low WF, the performance and the lifetime of a copper RF cavity are strongly affected by breakdown phenomena and thermal stress generated by electron emission from the surface [11]. A high WF conductive coating could be used to reduce these detrimental phenomena, extending the lifetime of the device and allowing it to operate at higher electric fields [1,5,11,12]. Hence, $MoO_3$ coating can significantly enhance the electronic and mechanical properties of copper-based devices via its high WF and relatively higher hardness, compared with copper [5,13–15], without affecting the surface conductivity. Because the thermal evaporation deposition produces disordered and poorly adhesive $MoO_3$ coatings [5], with the aim to obtain ordered $MoO_3$ coatings, we tried to optimize the annealing procedure. This method minimized the formation of $MoO_2$, which must be avoided, since the slightly off-axis position of Mo atoms in the $MoO_2$ phase causes the lowering of the WF (~4.6 eV) [3,16]. To establish the optimal annealing temperature for an ordered $MoO_3$ film on a copper substrate, we investigated the structural evolution of annealed $MoO_3$ films by X-ray Absorption Spectroscopy (XAF) in X-ray Absorption Near-Edge Structure (XANES) and in the Extended X-ray Absorption Fine Structure (EXAFS) regions [17–20].

## 2. Materials and Methods

Molybdenum trioxide films were deposited in a dedicated vacuum sublimation set up on 5 mm-thick copper substrates [16]. Molybdenum trioxide powder (99.97% trace metal basis, Sigma-Aldrich®, St. Louis, MO, USA) was heated up to 600 °C in a tungsten crucible inside the evaporation chamber with a base pressure of $10^{-5}$ mbar. In order to anneal the coating without oxidizing the copper substrate, a heat treatment in a low vacuum environment was performed, with a base pressure of $5 \times 10^{-1}$ mbar. We also considered a fast heating procedure to minimize the Mo reduction process and to further reduce copper oxidization. This setup allowed us to reach a temperature of up to 500 °C in less than 10 min, with a constant heating rate of ~1 °C/s. After a brief temperature decrease, the samples were exposed to air at 200 °C in order to increase the amount of oxygen in the film [16].

X-Ray Absorption Spectroscopy (XAS) measurements were performed at the B08 beamline at the European Synchrotron Radiation Facility (ESRF) in Grenoble, which works at the energy of 6 GeV and with a current of ~200 mA in the top-up mode. The B08 beamline is the Italian CRG (LISA), optimized for X-ray absorption measurements. Its optical layout covers a wide range of energies, from 5 to 40 keV, and, with the Si(111) crystals, delivers a flux to the sample of ~$10^{11}$ ph/s within a spot of ~200 μm [21]. The acquisition at the Mo K-edge (19,999 eV) spectra was performed in the energy step-scan mode, and the fluorescence signal was collected by a 12-element Ge detector. The measurements were carried out with an energy resolution in the order of 2 eV, and the scan steps were set to 0.5 eV and 1 eV in the XANES and the EXAFS region, respectively.

X-ray Absorption Spectroscopy (XAS) analysis were performed using the software package FEFF6 (Seattle, WA, USA) [22]. Background subtraction and normalization of the absorption spectra were performed by fitting the pre-edge region with a first-order polynomial, and the spectrum after the edge with a cubic polynomial. The Mo K edge absorption threshold was associated with the first maximum of the first derivative.

## 3. Results and Discussion

The comparison of XANES spectra at the Mo K edge of the 250 nm $MoO_3$ films deposited on a copper substrate and annealed at 300 °C, 350 °C, and 500 °C is shown in Figure 1, along with the $MoO_3$ reference spectrum. The latter has a well-defined pre-edge peak at 20,005.6 eV (peak A), with two other major components at 20,025.7 eV and 20,037.2 eV (peaks B and C). The broadened features of the as-deposited film, in comparison with the reference spectra of the α-$MoO_3$ spectrum, confirmed that this film was mainly disordered [23–25]. Within the initial annealing stage at 300 °C, the ordering process (flagged by peak C) started to appear, although the film remained disordered. Increasing the annealing temperature to 350 °C triggered an ordering process within the film, leading to the

observation of the typical $MoO_3$ features (peaks B and C). At the annealing temperature of 500 °C, the spectrum indicated the occurrence of a phase transformation: a clear shift of 3.8 eV of the third component at the energy of 20,033.4 eV (peak C) was observed. This dynamic can be also associated with the partial reduction of Mo ions due to oxygen loss [23,26,27]. A closer look to the XANES spectra also revealed changes in the pre-edge peak as a function of the annealing temperature. Above 350 °C, we observed a broadening and a lowering of the pre-edge component that can be associated with the partial reduction of $Mo^{6+}$ ions to $Mo^{4+}$. Indeed, the reduction of the pre-edge intensity, that is a probe of the local and partial empty density of states around Mo atoms, was due to the direct 1s to 4d quadrupole-allowed transitions and to the dipole-allowed 1s hybridized (5p,4d) states.

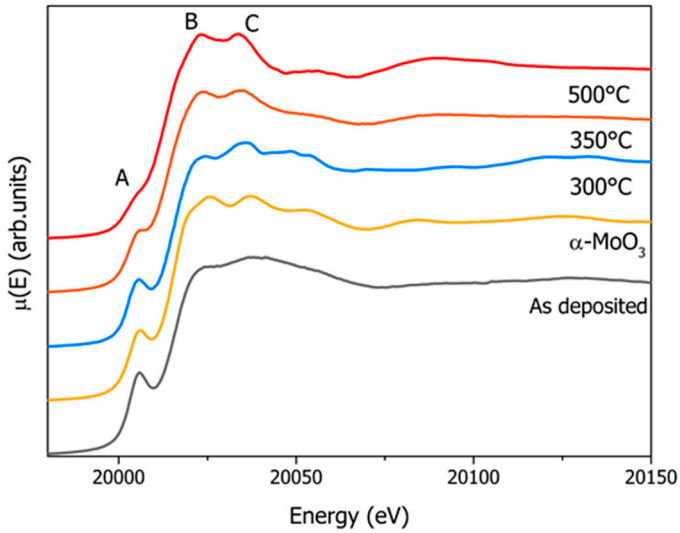


**Figure 1.** Comparison of X-ray Absorption Near-Edge Structure (XANES) spectra at the molybdenum K edge for the standard α-$MoO_3$ powder (yellow), the as-deposited $MoO_3$ film 250 nm thick (grey), and those annealed at 300 °C (blue), 350 °C (orange), and 500 °C (red).

In order to probe the dependence of the structural changes of these oxide films on the annealing temperature, a more detailed XAS analysis was carried out. Figure 2 shows the comparison of the pseudo-radial distribution of the distances in these samples, obtained from the Fourier transform (FT) of the EXAFS X(k) from the as-deposited film, the annealed samples, and the α-$MoO_3$ reference.

The as-deposited film and the one annealed at 300 °C exhibited only a large peak at around 1.7 Å, corresponding to the nearest oxygen neighbors (Mo–O) without additional shells. This is in agreement with previous XANES spectra of these same samples that pointed out the presence of disordered phases [23]. On the other hand, a structural ordering of the coating was observed at higher annealing temperatures (> 350 °C). As shown in Figure 2, at 350 °C, a split of the first peak appeared, similar to the spectrum of the reference, and a second major component associated with the nearest Mo neighbors (Mo–Mo second shell distance) also emerged at around 3.5 Å. A comparison with the α-$MoO_3$ spectrum confirmed the formation of the dominant $MoO_3$ phase, in agreement with the XANES spectra. At 500 °C, the FT was different from that of the film annealed at 350 °C, showing a single strong peak due to changes in the first Mo–O shells and in good agreement with the FT of the $MoO_2$ phase [27]. The Mo–Mo peak at the distance of ~2.5 Å also appeared, in agreement with the edge-sharing octahedra characteristic of the distorted rutile structure of the $MoO_2$ phase [27].

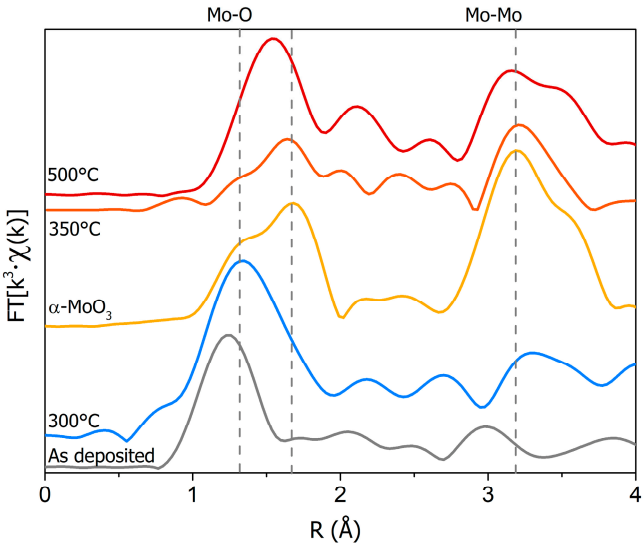


**Figure 2.** Fourier transform (FT) of the $k^3 \cdot X(k)$ signal among the disordered $MoO_3$ film (gray), the $\alpha$-$MoO_3$ (yellow), the 300 °C (blue), 350 °C (orange), and 500 °C (red) annealed $MoO_3$ films deposited on Cu and the $\alpha$-$MoO_3$ powder (yellow). The vertical continuous lines refer to the position of $MoO_3$ main peaks. It is clear that at 500 °C, the distribution is mainly related to $MoO_2$, while at 350 °C, it corresponds to the $\alpha$-$MoO_3$ phase.

The EXAFS data of the $\alpha$-$MoO_3$ reference and annealed films were fitted using the FEFF package with $MoO_3$ and $MoO_2$ reference crystalline structures, respectively (see Figure 3). Structural refinements were performed by minimizing the difference of the raw absorption spectra with the simulation, including the structural oscillations, $\chi(\kappa)$, and a suitable background function. The fit was performed in two steps: first, the $E_0$ and $S_0^2$ parameters fitting only the first shell were calculated. In the second step, only the distances (R) and $\sigma^2$ were left free. During this procedure, we used constant coordination numbers obtained from $MoO_3$ and $MoO_2$ crystal structures. The results (see Table 1) of the 350 °C annealed sample returned distances in good agreement with the $\alpha$-$MoO_3$ structure, with a reasonable mean-square relative displacement ($\sigma^2$ = 0.0015 Å$^2$).

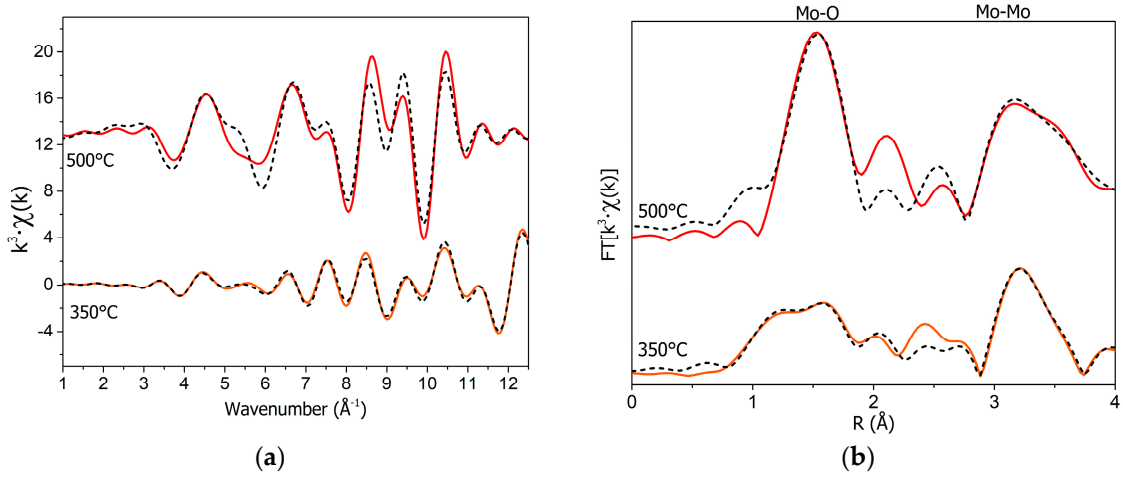


**Figure 3.** (**Left**) Comparison of the $k^3 \cdot X(k)$ and the FT (**right**) of annealed $MoO_3$ films deposited on Cu at 350 °C (orange) and 500 °C (red). Corresponding fits are the black dashed lines. The 350 °C signal was fitted with the $\alpha$-$MoO_3$ structure, while the 500 °C signal was fitted with the orthorhombic $MoO_2$ structure.

**Table 1.** Best-fit values of the samples from Extended X-ray Absorption Fine Structure (EXAFS) spectra. For the 350 °C sample, the fit was obtained from a refinement of the sum of theoretical EXAFS calculated for the orthorhombic $MoO_3$ structure (k range = 3–12.5 $Å^{-1}$, R = 0.5–4.2 Å, 8 single scattering paths, 16 free parameters, and two fixed, r-factor = 0.027, $S_0{}^2$ = 0.6) and a monoclinic $MoO_2$ structure for the 500 °C sample (k range = 3–12.5 $Å^{-1}$, R = 0.5–4.2 Å, 6 single scattering paths, 12 free parameters, and two fixed, r-factor = 0.021, $S_0{}^2$ = 0.8). The coordination numbers are those of the $MoO_3$ and $MoO_2$ structures.

| **α-$MoO_3$ Reference** | | | | **350 °C Annealing** | | | | **500 °C Annealing** | | | |
|---|---|---|---|---|---|---|---|---|---|---|---|
| **Shell** | CN | R(Å) | $\sigma^2$(Å$^2$) | **Shell** | CN | R(Å) | $\sigma^2$(Å$^2$) | **Shell** | CN | R(Å) | $\sigma^2$(Å$^2$) |
| **Mo-O** | 1 | 1.70 ± 0.05 | 0.0024 ± 0.0004 | **Mo-O** | 1 | 1.70 ± 0.08 | 0.0015 ± 0.0012 | **Mo-O** | 2 | 1.99 ± 0.07 | 0.0037 ± 0.0011 |
| **Mo-O** | 1 | 1.78 ± 0.10 | 0.0023 ± 0.0003 | **Mo-O** | 1 | 1.80 ± 0.08 | 0.0013 ± 0.0004 | **Mo-O** | 4 | 2.02 ± 0.05 | 0.0031 ± 0.0016 |
| **Mo-O** | 2 | 1.99 ± 0.06 | 0.0025 ± 0.0002 | **Mo-O** | 2 | 2.07 ± 0.10 | 0.0021 ± 0.0010 | **Mo-Mo** | 2 | 3.17 ± 0.06 | 0.0041 ± 0.0012 |
| **Mo-O** | 1 | 2.22 ± 0.04 | 0.0022 ± 0.0004 | **Mo-O** | 1 | 2.22 ± 0.11 | 0.0022 ± 0.0017 | **Mo-O** | 4 | 3.42 ± 0.05 | 0.0029 ± 0.0010 |
| **Mo-O** | 1 | 2.31 ± 0.03 | 0.0022 ± 0.0003 | **Mo-O** | 1 | 2.30 ± 0.05 | 0.0016 ± 0.0009 | **Mo-Mo** | 8 | 3.73 ± 0.07 | 0.0037 ± 0.0007 |
| **Mo-Mo** | 2 | 3.41 ± 0.03 | 0.0027 ± 0.0003 | **Mo-Mo** | 2 | 3.38 ± 0.05 | 0.0027 ± 0.0002 | **Mo-O** | 4 | 4.05 ± 0.08 | 0.0035 ± 0.0005 |
| **Mo-Mo** | 2 | 3.75 ± 0.02 | 0.0025 ± 0.0002 | **Mo-Mo** | 2 | 3.73 ± 0.10 | 0.0019 ± 0.0002 | | | | |
| **Mo-Mo** | 2 | 4.02 ± 0.09 | 0.0025 ± 0.0010 | **Mo-Mo** | 2 | 4.08 ± 0.04 | 0.0019 ± 0.0005 | | | | |

On the contrary, the fit of the sample annealed at 500 °C showed a dominant $MoO_2$ phase, with only the distances of the $MoO_2$ structure ruling out the contribution of $MoO_3$ phases. The small deviations of the fit from the experimental spectrum can be associated with the presence of minor amounts of other non-stoichiometric oxide phases.

## 4. Conclusions

The structural evolution of $MoO_3$ films deposited on copper after annealing was investigated with XAS spectroscopy. At lower annealing temperatures, the experimental spectra did not change, showing that the as-deposited films were disordered up to ~300 °C. For the annealing procedure in a low vacuum regime (0.5 mbar) at around 350 °C, the spectra shows that the film underwent an ordering process, with the formation of the α-$MoO_3$ phase, as confirmed by the EXAFS analysis. Moreover, XANES spectra at 500 °C showed that the molybdenum ions underwent a decrease of the pre-edge intensity, in agreement with a reduction from a$Mo^{6+}$ to a $Mo^{4+}$ valence state. The fit of the EXAFS spectra showed that the phase of these films could be mainly associated with the presence of the $MoO_2$ phase. These results represent a first important advancement for many foreseen applications of these coatings, in particular for compact RF devices made of copper.

**Author Contributions:** Conceptualization, methodology, S.M., A.M., and I.D.; data analysis, S.M., J.R., and G.C.; Manuscript preparation: S.M., A.M., and J.R.; S.M., A.M., J.R., I.D., G.C., B.S., J.S., L.F. have reviewed the manuscript.

**Funding:** We acknowledge the INFN for the support within DEMETRA and NUCLEAAR, two projects funded by the INFN Vth Committee. We also acknowledge the financial support of the Bilateral Cooperation Agreement between Italy and Japan of the *Italian Ministry of Foreign Affairs and of the International Cooperation* (MAECI) in the framework of the project of major relevance N. PGR0072.

**Acknowledgments:** We acknowledge ESRF and CNR-IOM for providing beamtime (proposal n. 08-01 1056) at LISA, the Italian beamline at ESRF. We acknowledge A. Bianconi for many fruitful discussions and P. De Padova and M. Lucci for their contribution to the development of the annealing procedure and to the experimental setup.

**Conflicts of Interest:** The authors declare no conflict of interest.

## References

1. Guo, Y.; Robertson, J. Origin of the high work function and high conductivity of $MoO_3$. *Appl. Phys. Lett.* **2014**, *105*, 222110. [CrossRef]
2. Meyer, J.; Hamwi, S.; Kröger, M.; Kowalsky, W.; Riedl, T.; Kahn, A. Transition metal oxides for organic electronics: energetics, device physics and applications. *Adv. Mater.* **2012**, *24*, 5408–5427. [CrossRef]

3. Scanlon, D.O.; Watson, G.W.; Payne, D.J.; Atkinson, G.R.; Egdell, R.G.; Law, D.S.L. Theoretical and experimental study of the electronic structures of $MoO_3$ and $MoO_2$. *J. Phys. Chem. C* **2010**, *114*, 4636–4645. [CrossRef]
4. Hanson, E.D.; Lajaunie, L.; Hao, S.; Myers, B.D.; Shi, F.; Murthy, A.A.; Dravid, V.P. Systematic study of oxygen vacancy tunable transport properties of few-layer $MoO_{3-x}$ enabled by vapor-based synthesis. *Adv. Funct. Mater.* **2017**, *27*, 1605380. [CrossRef]
5. Macis, S.; Aramo, C.; Bonavolontà, C.; Cibin, G.; D'Elia, A.I.; Davoli, M.; De Lucia, M.; Lucci, S.; Lupi, M.; Miliucci, A.; et al. $MoO_3$ films Grown on polycrystalline Cu: Morphological, structural, and electronic properties. *J. Vac. Sci. Technol. A* **2019**, *37*, 021513. [CrossRef]
6. De Castro, I.A.; Datta, R.S.; Ou, J.Z.; Castellanos-Gomez, A.S.; Sriram, T.D.; Kalantar-zadeh, K. Molybdenum oxides–from fundamentals to functionality. *Adv. Mat.* **2017**, *29*, 1701619. [CrossRef]
7. Greiner, M.T.; Chai, L.; Helander, M.G.; Tang, W.; Lu, Z.H. Metal/metal-oxide interfaces: How metal contacts affect the work function and band structure of $MoO_3$. *Adv. Funct. Mater.* **2013**, *23*, 215–226. [CrossRef]
8. Lambert, D.S.; Lennon, A.; Burr, P.A. Extrinsic defects in crystalline $MoO_3$: Solubility and effect on the electronic structure. *J. Phys. Chem. C* **2018**, *122*, 27241–27249. [CrossRef]
9. Lambert, D.S.; Murphy, S.T.; Lennon, A.; Burr, P.A. Formation of intrinsic and silicon defects in $MoO_3$ under varied oxygen partial pressure and temperature conditions: An ab initio DFT investigation. *RSC Adv.* **2017**, *7*, 53810–53821. [CrossRef]
10. Akande, S.O.; Chroneos, A.; Vasilopoulou, M.; Kennou, S.; Schwingenschlögl, U. Vacancy formation in $MoO_3$: Hybrid density functional theory and photoemission experiments. *J. Mater. Chem. C* **2016**, *4*, 9526–9531. [CrossRef]
11. Castorina, G.; Marcelli, A.; Monforte, F.; Sarti, S.; Spataro, B. An analytical model for evaluation of the properties of metallic coatings in RF structures. *Condens. Matter* **2016**, *1*, 12. [CrossRef]
12. Marcelli, A.; Spataro, B.; Sarti, S.; Dolgashev, V.A.; Tantawi, S.; Yeremian, D.A.; Higashi, Y.; Parodi, R.; Notargiacomo, A.; Junqing, X.G.; et al. Characterization of thick conducting molybdenum films: Enhanced conductivity via thermal annealing. *Surf. Coat. Tech.* **2015**, *261*, 391–397. [CrossRef]
13. Xu, Y.; Spataro, B.; Sarti, S.; Dolgashev, V.A.; Tantawi, S.; Yeremian, A.D.; Higashi, Y.; Grimaldi, M.G.; Romano, L.; Ruffino, F. Structural and morphological characterization of Mo coatings for high gradient accelerating structures. *J. Phys. Conf. Ser.* **2013**, *430*, 012091. [CrossRef]
14. Marcelli, A.; Spataro, B.; Castorina, G.; Xu, W.; Sarti, S.; Monforte, F.; Cibin, G. Materials and breakdown phenomena: Heterogeneous molybdenum metallic films. *Condens. Matter* **2017**, *2*, 18. [CrossRef]
15. Dolgashev, V.A.; Tantawi, S.G.; Park, M.; Higashi, Y.; Spataro, B. Study of basic Rf breakdown phenomena in high gradient vacuum structures. In Proceedings of the 16th International Linear Accelerator Conference LINAC2010, Tsukuba, Japan, 12–17 September 2010; pp. 1043–1047.
16. Macis, S. Deposition and Characterization of Thin $MoO_3$ Films on Cu for Technological Applications. Ph.D. Thesis, Roma Tor Vergata University, Roma, Italy, 2019.
17. Bianconi, A.; Marcelli, A. Surface X-Ray Absorption near-edge structure: XANES. In *Synchrotron Radiation Research. Advances in Surface Science*; Bachrach, R.Z., Ed.; Plenum Press: New York, NY, USA, 1992; Chapter 2; Volume 1.
18. Marcelli, A. Phase separations in highly correlated materials. *Acta Phys. Polonica A* **2016**, *129*, 264–269. [CrossRef]
19. Garcia, J.; Benfatto, M.; Natoli, C.R.; Bianconi, A.; Davoli, I.; Marcelli, A. Three particle correlation function of metal ions in tetrahedral coordination determined by XANES. *Solid State Commun.* **1986**, *58*, 595–599. [CrossRef]
20. Giuli, G.; Paris, E.; Wu, Z.; Brigatti, M.F.; Cibin, G.; Mottana, A.; Marcelli, A. Experimental and theoretical XANES and EXAFS study of tetra-ferriphlogopit. *Eur. J. Miner.* **2001**, *13*, 1099–1108. [CrossRef]
21. d'Acapito, F.; Lepore, G.O.; Puri, A.; Laloni, A.; la Manna, F.; Dettona, E.; de Luisa, A.; Martin, A. The LISA beamline at ESRF. *J. Synchrotron Radiat.* **2019**, *26*, 551–558.
22. Zabinsky, S.I.; Rehr, J.J.; Ankudinov, A.; Albers, R.C.; Eller, M.J. Multiple scattering calculations of X-ray absorption spectra. *Phys. Rev. B* **1995**, *52*, 2995. [CrossRef]
23. Kopachevska, N.S.; Melnyk, A.K.; Bacherikova, I.V.; Zazhigalov, V.A.; Wieczorek-Ciurowa, K. Determination of molybdenum oxidation state on the mechanochemically treated $MoO_3$. *Хіміяфізиката Технологія Поверхні* **2015**, *6*, 474–480, ISSN 2079-1704.

24. Di Cicco, A.; Bianconi, A.; Coluzza, C.; Rudolf, P.; Lagarde, P.; Flank, A.M.; Marcelli, A. XANES study of structural disorder in amorphous silicon. *J. Non-Cryst. Solids* **1990**, *116*, 27–32. [CrossRef]
25. Bianconi, A.; Garcia, J.; Marcelli, A.; Benfatto, M.; Natoli, C.R.; Davoli, I. Probing higher order correlation functions in liquids by XANES (X-ray absorption Near Edge Structure). *J. Phys. Colloq.* **1985**, *46*, 101–106. [CrossRef]
26. Ressler, T.; Jentoft, R.E.; Wienold, J.; Gu1nter, M.M.; Timpe, O. In situ XAS and XRD studies on the formation of Mo suboxides during reduction of $MoO_3$. *J. Phys. Chem. B* **2000**, *104*, 6360–6370. [CrossRef]
27. Ressler, T.; Wienold, J.; Jentoft, R.E. Formation of bronzes during temperature-programmed reduction of $MoO_3$ with hydrogen—An in situ XRD and XAFS study. *Solid State Ion.* **2001**, *141*, 243–251. [CrossRef]